

# Hydrogen effect on the field dependence of Young's modulus of FeCuNbSiB alloy

V.S. Kolat, N. Bayri, S. Atalay\*

Physics Department, Science and Arts Faculty, Inonu University, 44069 Malatya, Turkey

Received 28 January 2002; received in revised form 26 February 2002; accepted 26 February 2002

## Abstract

The magnitude of the magnetic field dependence of Young's modulus of FeCuNbSiB alloys was found to decrease after hydrogenation but to nearly recover after 2–3 h. A large variation in the magnetic and the magnetoelastic properties of as-received sample was observed after hydrogenation.  $\Delta E$  and  $M-H$  results of samples annealed at 450 °C showed that annealing could reduce hydrogen permeation into the sample. Practically no variation in the magnetic and magnetoelastic properties of samples annealed at 550 °C were observed before and after hydrogenation.

© 2002 Elsevier Science B.V. All rights reserved.

**Keywords:** Transition metal compounds; Amorphous materials; Gas–solid reaction; Magnetization measurements

## 1. Introduction

Fe-based nanocrystalline alloys obtained by controlled partial crystallisation of some Fe–Cu–Nb–Si–B amorphous alloys have been studied extensively because of their excellent soft magnetic properties [1–3]. Since the soft magnetic amorphous and nanocrystalline Fe–Cu–Si–Nb–B alloys have gained acceptance for industrial applications, investigation of their magnetic and magnetoelastic altering upon hydrogenation is not only practical but could also be useful to further understand the amorphous structure.

Previously, the effect of hydrogen charging on the properties of amorphous alloys has been studied by many scientists [4–8]. It has been reported that hydrogen can lead to important modifications in the electronic structure, which consequently changes magnetic and mechanical properties of the materials [9–14]. Up to now, no study about the effect of hydrogen charging on the magnetoelastic properties of amorphous and nanocrystalline Fe–Cu–Si–Nb–B alloys has been reported. In this work, we therefore present a study of the effect of hydrogen charging

on magnetic and magnetoelastic properties of Fe–Cu–Nb–Si–B amorphous and nanocrystalline alloys.

## 2. Experimental

Fe<sub>73.5</sub>Cu<sub>1</sub>Nb<sub>3</sub>Si<sub>13.5</sub>B<sub>9</sub> amorphous alloys were produced by a melt-spinning method. The samples were cut into sizes 4 cm long and 0.5 cm wide and with a thickness of  $23 \pm 2$   $\mu\text{m}$ . The samples were annealed under an argon atmosphere for 1 h at temperatures ranging from 400 to 650 °C. Hydrogen was charged cathodically for 30 min with the cathodic current density of 50  $\text{A m}^{-2}$  in all samples using 0.5 M  $\text{H}_2\text{SO}_4$  solution with 0.1  $\text{g l}^{-1}$   $\text{As}_2\text{O}_3$  as a poison and the total area of the sample in the charging process was kept at about 1.2  $\text{cm}^2$ . The structure of samples was investigated using X-ray diffraction (Rigaku-Radb) system and no change in the sample structure before and after hydrogenation was detected. The magnetization ( $M-H$ ) curves were measured in ac mode (50 Hz). Magnetostriction measurements were performed using a fibre-optic dilatometer system. The magnetic field dependence of Young's modulus ( $\Delta E$  effect) was measured by the vibrating reed method. The third mode was excited with a free length of 2 cm. The values of Young's modulus

\*Corresponding author. Tel.: +90-422-341-0010; fax: +90-422-341-0010.

E-mail address: [satalay@inonu.edu.tr](mailto:satalay@inonu.edu.tr) (S. Atalay).

are normalised to the modulus value,  $E_o$ , at  $H = 0$  applied field or  $E_s$ , the modulus value at maximum applied field.

### 3. Results and discussion

Fig. 1 shows the variation of Young's modulus of as-received samples as a function of hydrogen desorption time at  $H = 0$ . It can be seen that hydrogenation increases the value of Young's modulus which recovers gradually with the evolving of hydrogen, but it could only return to the 235 GPa value after 24 h. The Young's modulus of the sample can be written as the following expression [15]:

$$E = \frac{\pi\mu L^4}{4\alpha_n^4 r^4} f^2 \quad (1)$$

where  $\mu$  is the mass per unit length of the sample and the typical value for  $\mu$  in our experiments is about  $0.0037 \text{ g cm}^{-1}$ ,  $r$  is the thickness of the sample,  $L$  is the length of the sample,  $\alpha_n$  is the vibration mode parameter and  $f$  is the resonant frequency. It is well known that hydrogen charging could change the length of the sample [10]. According to Eq. (1),  $E$  is proportional to  $L^4$ . It can therefore be assumed that the main contribution to the change in the  $E$  value with hydrogenation is due to variation in the sample length. This partly irreversible process in the Young's modulus upon hydrogenation can also be partly related to two kinds of phenomena: plastic deformation induced by the internal stresses produced by hydrogen and permanent local damages produced by bubbles that appear by hydrogen accumulation in the sample defects.

The crystallisation temperature of Fe–Cu–Si–Nb–B sample was determined by DTA to be  $520^\circ\text{C}$  at a heating rate of  $10^\circ\text{C min}^{-1}$ . Therefore, the annealing temperatures were chosen just below and above the crystallisation temperature. X-ray results indicated that the sample an-

nealed at  $450^\circ\text{C}$  has a fully amorphous structure. Annealing between  $525$  and  $600^\circ\text{C}$  leads to the formation of  $\alpha\text{-Fe(Si)}$  crystallites in amorphous matrix. The average grain size of  $\alpha\text{-Fe(Si)}$  crystallites is about  $13\text{--}15 \text{ nm}$  for the sample annealed at  $550^\circ\text{C}$ . The sample annealed at  $650^\circ\text{C}$  or at higher temperatures showed nearly full crystallisation. In this sample  $\alpha\text{-Fe(Si)}$ ,  $\text{Fe}_3\text{Si}$ ,  $\text{Fe}_2\text{B}$  phases were observed.

It was observed that both  $H_c$  and magnetostriction values of the samples annealed between  $450$  and  $550^\circ\text{C}$  decrease due to the formation of the  $\alpha\text{-FeSi}$  phase. Fig. 2 shows the field dependence of the normalised Young's modulus ( $\Delta E$  effect) for as-received and annealed samples. This results are in agreement with the previously reported  $\Delta E$  results [16]. The magnitude of  $\Delta E$  effect increases from as-received state ( $\sim 6\%$ ) to a maximum of about  $47\%$  at an annealing temperature of  $450^\circ\text{C}$ . Annealing at  $550^\circ\text{C}$  leads to a large decrease in the magnitude of  $\Delta E$  effect.

For amorphous materials, the magnitude of the  $\Delta E$  effect, expressed by the  $E_{\min}/E_s$  ratio, is determined by the dimensionless quantity  $\beta = \lambda_s^2 E_s / K$ , where  $K$  is the anisotropy constant [16]. It can be shown that  $\beta = (E_s/E - 1)/F$ , where  $F$  is a function of easy axis distribution and applied field. For data considered in this study,  $F$  can be taken to be about 1. In this study we use  $E_{\min}/E_s$  ratio to follow the change in  $\beta$  and hence,  $K$ . For the amorphous and the nanocrystalline materials, the basic anisotropy contributions are:

1. The magneto-elastic anisotropy,  $K_\sigma = 3/2 \lambda_s \sigma$ , where  $\sigma$  is the internal stress.
2. Shape anisotropy,  $K_D = 1/2 D \mu_0 M_s^2$ , where  $D$  is the shape demagnetization factor.
3. The magneto-crystalline anisotropy,  $K_c$ , if there is any.

In as-received state  $K_D$  is very small compared to  $K_\sigma$  and  $K_c = 0$ . As-received samples have large internal stress,

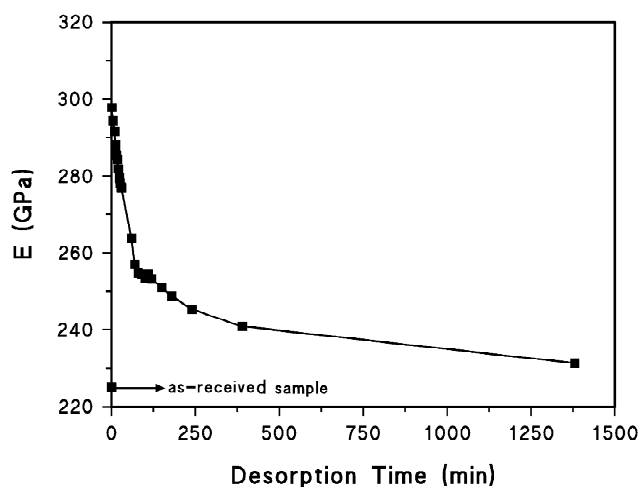


Fig. 1. The variation of Young's modulus as a function of hydrogen desorption time.

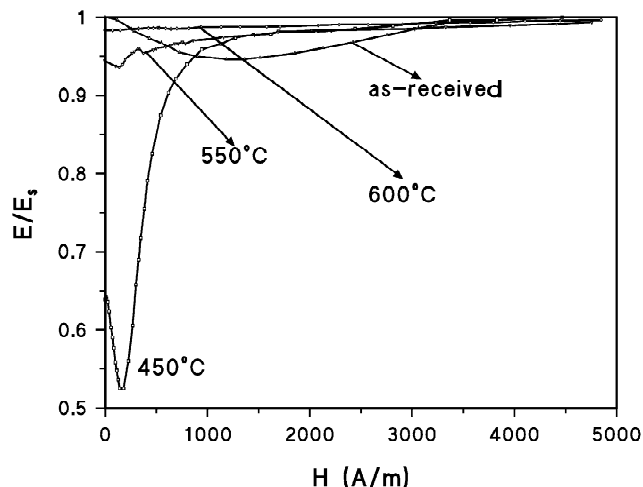


Fig. 2. The field dependence of normalised Young's modulus of as-received and annealed samples at various temperatures.

which combines with magnetostriction to produce very high anisotropy,  $K_\sigma$  ( $\lambda_s$  is about  $24 \times 10^{-6}$  for the as-received sample). Therefore, the  $\Delta E$  effect for the as-received sample is very small and  $\beta$  is about 0.02. Annealing up to  $500^\circ\text{C}$  relieves the internal stresses, thus reducing  $K_\sigma$ , hence increasing the magnitude of  $\Delta E$  effect. Annealing above  $600^\circ\text{C}$  causes an increase in the amount of the  $\text{Fe}_2\text{B}$  phase, leading to a large increase in  $K_c$ , and hence to the total  $K$ . This then leads to a sharp decrease in the magnitude of the  $\Delta E$  effect. For annealing temperatures between  $500$  and  $600^\circ\text{C}$ , where nanocrystallisation occurs, the mechanism is slightly different. It is also interesting that  $\lambda_s$  decreases at this annealing temperature range due to formation of the negatively magnetostrictive  $\alpha\text{-FeSi}$  phase. It has been reported that with the formation of the nanocrystalline  $\alpha\text{-FeSi}$  phase in amorphous alloys, the average  $K$  value decreases by a large amount. For nanocrystalline Finemet alloy, a typical  $K$  value can be as low as  $1\text{--}4 \text{ J m}^{-3}$  [1,2]. For sample annealed at  $500^\circ\text{C}$ , taking  $E_s = 17 \times 10^{10} \text{ N m}^{-2}$ ,  $\lambda_s \sim 10 \times 10^{-6}$  one can deduce from these equations:  $\beta = \lambda_s^2 E_s / K$ ,  $\beta = (E_s / E - 1) / F$ , that  $K \sim 17 \text{ J m}^{-3}$ . For the sample annealed at  $550^\circ\text{C}$ , the  $K$  value is found to be about  $15 \text{ J m}^{-3}$ . This value of  $K$  for the sample annealed at  $550^\circ\text{C}$  is found to be slightly higher than previously reported values. For nanocrystalline samples,  $\lambda_s$  is very small, therefore, the contribution of  $K_\sigma$  to  $K$  is nearly zero. The main contribution to  $K$  comes from  $K_c$ .

Figs. 3 and 4 show the  $\Delta E$  effect curves during hydrogen evolution for the as-received sample and the sample annealed at  $450^\circ\text{C}$ , respectively. The  $\Delta E$  effect results reveal that the hydrogen atoms charged into the amorphous  $\text{Fe-Cu-Si-Nb-B}$  could change the magnitude of the  $\Delta E$  curves and put the sample in a very unstable state. When the hydrogenated sample was left in air, hydrogen atoms leave the sample very quickly during the

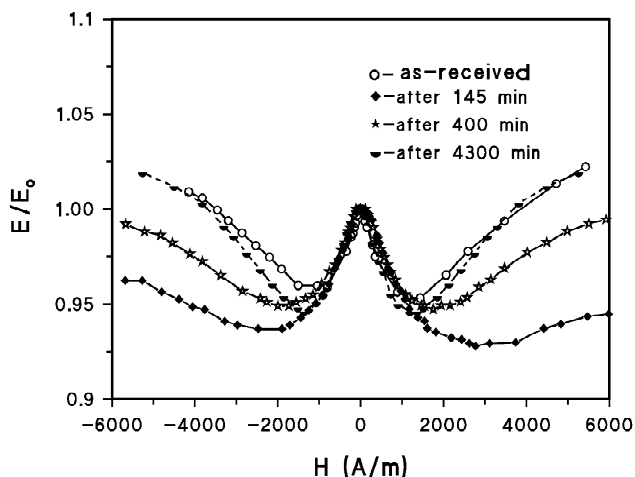


Fig. 3. The variation of normalised Young's modulus with applied field during hydrogen degassing time for as-received sample.

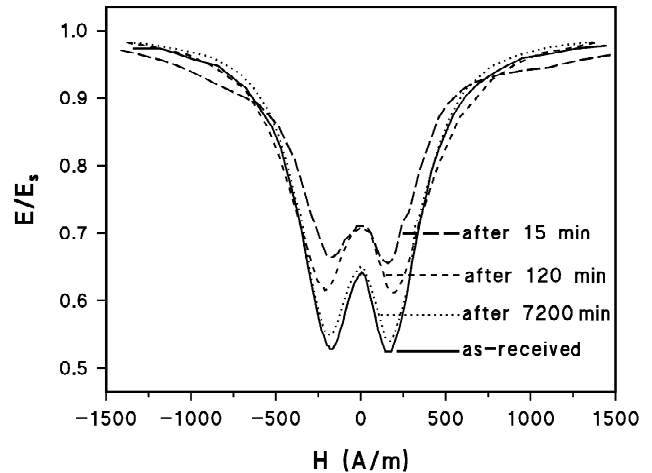


Fig. 4. Normalised Young's modulus against applied field for annealed sample at  $450^\circ\text{C}$  while hydrogen is leaving the sample.

initial 1–3 h than it slows down. Also the measured  $M\text{--}H$  curves support this behaviour (Figs. 5 and 6).

It was found that the shapes of the  $E/E_s$  curves are very similar to each other during hydrogen desorption.  $E_{\min}$  was observed in all the  $\Delta E$  curves. According to the Squire model [17], the average easy axis angle of magnetization is between  $50$  and  $75^\circ$  with respect to ribbon axis. But, large variations in the magnitude of the  $\Delta E$  effect were observed with hydrogenation both in the as-received sample and sample annealed at  $450^\circ\text{C}$ . As it has been stated, the magnitude of  $\Delta E$  is determined by  $\beta = \lambda_s^2 E_s / K$ . It is also well known that hydrogenation induces very large internal stresses, the coupling of the internal stress with magnetostriction increases the magneto-elastic anisotropy constant,  $K_\sigma$ , and therefore  $K$ . So, the magnitude of  $\Delta E$  (or  $E_{\min}/E_s$  ratio) becomes smaller after hydrogenation. During hydrogen evolution,  $K_\sigma$  becomes smaller and the  $\Delta E$  curves nearly regain their previous shape. But small variations in

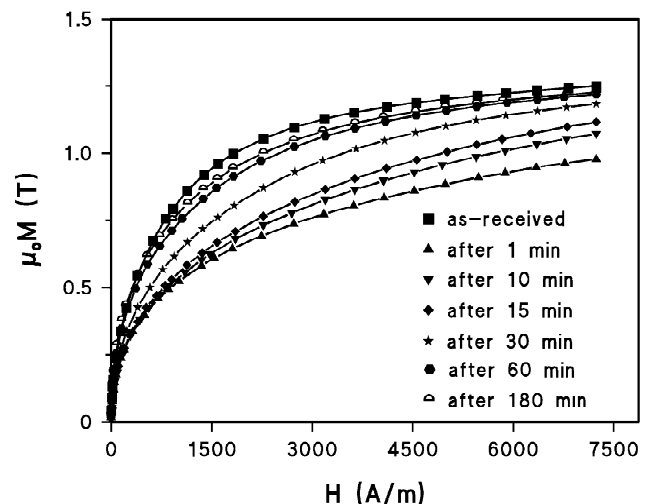


Fig. 5. Magnetization curves of hydrogenated as-received samples while hydrogen is leaving the sample.

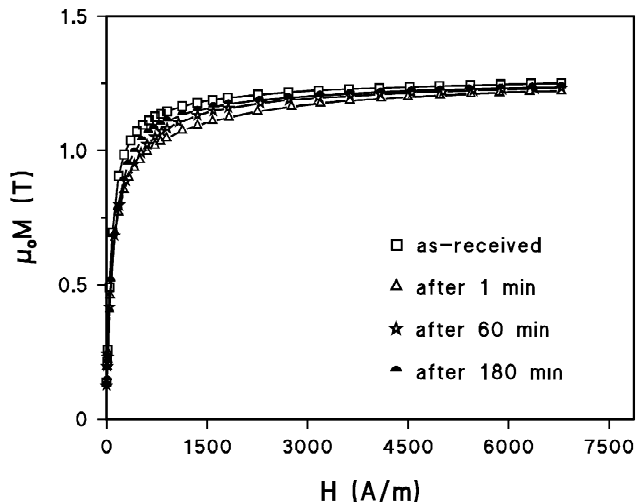


Fig. 6. Magnetization curves of hydrogenated sample annealed at 450 °C while hydrogen is leaving the sample.

the curves show the existence of some permanent plastic deformation. It was also found that the magnitude of  $\Delta E$  or the shape of the  $M-H$  curves in the as-received sample are more affected than in the sample annealed at 450 °C. Annealing of the sample increases the surface potential energy and lowers free volume; both effects decrease the hydrogen permeation into the amorphous ribbon [18,19]. As a result, for the sample annealed at 450 °C small differences were observed in the magnetic and magnetoelastic properties before and after hydrogen charging. The X-ray results did not show any surface oxidation, but this subject needs further study.

Previous studies have showed that nanocrystalline materials consist of two phases, amorphous and crystalline [1,2]. The formation of crystallisation in the amorphous bulk increases the surface roughness and consequently decreases surface potential energy [7]. Therefore, one can expect a larger hydrogen permeation into sample. But, the magnetostriction value of sample annealed at 550 °C is very small at about 2–3 ppm. Therefore, hydrogenation of nanocrystalline sample does not cause a large change  $K_\sigma = 3/2\lambda_s\sigma$  and  $K$ . Consequently, nearly no variations in the  $M-H$  and  $\Delta E$  curves of this sample were observed.

#### 4. Conclusions

The hydrogen charging effect on the magnetic and magnetoelastic properties of amorphous alloys seems to be

caused by mechanical stresses produced by plastic deformation and bubbles that appear due to hydrogen accumulation in defects. The coupling of the induced mechanical stresses with the magnetostriction of the samples produces a large anisotropy and a magnetic hardening, which decreases the magnitude of the  $\Delta E$  effect. These effects disappear after hydrogen is removed from the sample and the  $\Delta E$  and  $M-H$  curves show nearly reversible behaviour. The  $\Delta E$  and  $M-H$  results of samples annealed at 450 °C showed that annealing could reduce hydrogen permeation into the sample. No variation in the magnetic and magnetoelastic properties of sample annealed at 550 °C were observed.

#### Acknowledgements

This work has been supported by TUBITAK with project number TBAG-1832.

#### References

- [1] G. Herzer, Phys. Scripta T49 (1993) 307.
- [2] G. Herzer, Mater. Sci. Eng. A 133 (1991) 1.
- [3] S. Atalay, H.I. Adiguzel, P.T. Squire, P. Sovak, Mater. Sci. Eng. A 304–306 (2001) 918.
- [4] D.S. dos Santos, R.S. De Biasi, P.E.V. de Miranda, Mater. Sci. Forum 269–272 (1998) 819.
- [5] M.G. Alvarez, S.M. Vazquez, J. Moya, H. Sirkin, Scripta Mater. 44 (2001) 507.
- [6] J.M.D. Coey, D. Ryan, J. Appl. Phys. 53 (1982) 7804.
- [7] V.V. Kondratyev, A.V. Gapontsev, A.N. Voloshinskii, A.G. Obukhov, N.I. Timofeyev, Int. J. Hydrogen Energy 24 (1999) 819.
- [8] Z.S. Wronski, A.H. Morrish, IEEE Trans. Magn. 19 (1983) 1895.
- [9] B.S. Berry, W.C. Pritchett, J. Appl. Phys. 52 (1981) 1865.
- [10] E.M. Alcalá, E. Lopez, C. Aroca, M.C. Sanchez, J. Appl. Phys. 81 (1997) 815.
- [11] L.V. Spivak, N.Y. Skryabina, Int. J. Hydrogen Energy 24 (1999) 795.
- [12] N.Y. Skryabina, N.V. Pimenova, A.S. Petrov, Int. J. Hydrogen Energy 24 (1999) 801.
- [13] K. Tanaka, Y. Hayashi, M. Kimura, M. Yamada, J. Alloys Comp. 253–254 (1997) 101.
- [14] M. Stancheva, S. Manev, D. Lazarov, J. Alloys Comp. 234 (1996) 251.
- [15] S. Atalay, PhD thesis, School of Physics, Bath University, Bath, UK, 1992.
- [16] Z. Kaczowski, G. Vlasak, P. Duhaj, J. Magn. Magn. Mater. 157–158 (1996) 199.
- [17] P.T. Squire, J. Magn. Magn. Mater. 140–144 (1995) 1829.
- [18] W. Chambron, F. Lançon, A. Chamberod, Scripta Metall. 18 (1984) 29.
- [19] J.S. Georgiev, L.A. Anestiev, J. Nucl. Mater. 249 (1997) 133.